*Year :* 2018

# Modèle spatio-temporel de dépôt de gadolinium dans les noyaux gris centraux après IRM cérébrales répétées avec produit de contraste linéaire

## Marie Guillaume

**UNIVERSITE DE LAUSANNE - FACULTE DE BIOLOGIE ET DE MEDECINE**
Service de radiodiagnostic et radiologie interventionnelle

# Modèle spatio-temporel de dépôt de gadolinium dans les noyaux gris centraux après IRM cérébrales répétées avec produit de contraste linéaire

THESE

Préparée sous la direction du Professeur Philippe Maeder
(Avec la co-direction du Docteur Joachim Son-Forget)

et présentée à la Faculté de biologie et de médecine de
l'Université de Lausanne pour l'obtention du grade de

DOCTEUR EN MEDECINE

par

Guillaume MARIE

Médecin diplômé de la Confédération Suisse
Originaire de Bolligen (Bern)

Lausanne
2018

Ecole Doctorale
Doctorat en médecine

# Imprimatur

Vu le rapport présenté par le jury d'examen, composé de

| | |
|---|---|
| **Directeur de thèse** | Monsieur le Professeur **Philippe Maeder** |
| **Co-Directeur de thèse** | Monsieur le Docteur **Joachim Son-Forget** |
| **Expert** | Monsieur le Professeur **Roy Daniel** |
| **Vice-Directeur de l'Ecole doctorale** | Monsieur le Professeur **John Prior** |

la Commission MD de l'Ecole doctorale autorise l'impression de la thèse de
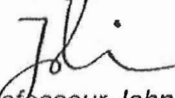
### Monsieur Guillaume MARIE

intitulée

### Modèle spatio-temporel de dépôt de gadolinium dans les noyaux gris centraux après IRM cérébrales répétées avec produit de contraste linéaire

Lausanne, le 20 septembre 2018

pour Le Doyen
de la Faculté de Biologie et de Médecine

Monsieur le Professeur John Prior
Vice-Directeur de l'Ecole doctorale

# Résumé

### Objectifs :

Le but de cette étude était d'évaluer systématiquement la modification spatiale et temporelle du signal au niveau des noyaux gris centraux des séquences T1 non contrastées d'IRM cérébrales chez des patients adultes ayant été exposés à au moins 10 doses consécutives de gadodiamide.

### Matériel et Méthode

Dans cette étude monocentrique rétrospective longitudinale, nous avons analysé les IRM cérébrales de 30 patients (12 femmes, 18 hommes ; âge moyen de 43 ans +- 11.6 ans) dont les images ont été acquises entre décembre 1998 et mars 2008. Nous avons tracé des régions d'intérêt dans le noyau denté, le globus pallidus, le putamen, le pulvinar, le noyau ventral postérieur du thalamus, le collicule supérieur, la substance noire et la substance blanche sur des séquences T1 non injectées. Chaque intensité de signal moyenne d'une région d'intérêt était normalisée par le signal moyen du pont. Les intensités moyennes normalisées étaient mesurées sur l'IRM baseline avant injection de gadodiamide puis sur chacune des 10 IRM successives. Nous avons utilisé des modèles linéaires à effets mixtes pour analyser les informations récoltées.

### Résultats :

Nous avons observé une augmentation linéaire significative du ratio d'intensité de signal sur les 10 administrations de gadodiamide (l'ensemble des noyaux de la base étudié était statistiquement significatif ($P<0.001$) à l'exception du thalamus ventral-postérieur avec $P<0.05$), avec l'augmentation la plus rapide de l'intensité de signal au niveau du noyau denté (B = 0.010), puis le globus pallidus (B = 0.0068), le putamen (B = 0.0063), le pulvinar (B = 0.0062), le collicule supérieur (B = 0.0057), la substance noire (B = 0.0034), et le noyau ventral-postérieur du thalamus (B = 0.0031). Au niveau de la substance blanche, aucune augmentation significative du signal a été observée ($P > 0.05$).

### CONCLUSIONS:

Plusieurs administrations consécutives de Gadodiamide sont associées à une augmentation du signal sur la séquence T1 sans injection de contraste, affichant un modèle graduel et non uniforme sur les différents noyaux de la base, entre autres le noyau ventral postérieur du thalamus qui était utilisé dans les précédentes études comme tissu de référence.

# Spatiotemporal Pattern of Gadodiamide-Related T1 Hyperintensity Increase Within the Deep Brain Nuclei

*Guillaume P.O. Marie, MD, Polona Pozeg, PhD, Reto A. Meuli, MD, PhD,*
*Philippe Maeder, MD, and Joachim Forget, MD, PhD*

**Objectives:** The purpose of the study was to systematically evaluate the precise spatial and temporal pattern of gadolinium-related changes in T1-weighted signal intensity on unenhanced magnetic resonance (MR) images, occurring in the deep brain nuclei of adult patients exposed to at least 10 consecutive doses of gadodiamide.

**Materials and Methods:** In this monocentric retrospective longitudinal study, we analyzed the brain MR images of 30 patients (12 women, 18 men; mean age, $43 \pm 11.6$ years) acquired between December 1998 and March 2008. We drew the regions of interest in the dentate nucleus, globus pallidus, putamen, pulvinar, ventral posterior nucleus of the thalamus, superior colliculus, substantia nigra, and white matter on unenhanced T1-weighted images. Each region of interest's mean signal intensity was normalized by the mean intensity of the pons. The normalized signal intensities were measured at the baseline before first gadodiamide administration and at each of 10 successive MR imaging examinations. We used linear mixed effects models to analyze the data.

**Results:** We observed a significant linear increase of signal intensity ratios across 10 successive gadodiamide administrations (all basal nuclei were significant at $P < 0.001$, except the ventral posterior thalamus, where $P < 0.05$), with the fastest signal intensity increase in the dentate nucleus (B = 0.010), followed by the globus pallidus (B = 0.0068), putamen (B = 0.0063), pulvinar (B = 0.0062), superior colliculus (B = 0.0057), substantia nigra (B = 0.0034), and ventral posterior nucleus of the thalamus (B = 0.0031). No significant signal increase was observed in the white matter ($P > 0.05$).

**Conclusions:** Multiple consecutive administration of gadodiamide is associated with an increase in T1-weighted hypersignal on the unenhanced scans, displaying a gradual and nonuniform pattern across different deep brain nuclei, including the ventral posterior thalamus, which was used as a reference tissue in previous studies.

**Key Words:** gadolinium retention, magnetic resonance imaging, deep brain nuclei, T1-weighted hyperintensity, gadodiamide

(*Invest Radiol* 2018;53: 748–754)

G adolinium-based contrast agents (GBCAs) are widely used in magnetic resonance (MR) imaging due to gadolinium's excellent paramagnetic properties, which improve visualization of blood-brain barrier disruption and hypervascularity. The GBCAs are classified into linear or macrocyclic agents based on the ligand's structure or into ionic or nonionic agents based on their charge. Their in vitro and in vivo stabilities differ, with macrocyclic GBCAs being kinetically more stable than linear GBCAs, and ionic linear GBCAs being thermodynamically more stable than nonionic linear agents.[1,2] Gadolinium-based contrast agent use was initially assumed to be safe until 2006, when the role of linear GBCAs in the genesis of nephrogenic systemic fibrosis in patients with renal failure was reported,[3] resulting in the restriction of linear agents to patients with normal renal function.

Recently, new data emerged, suggesting that gadolinium deposits in the brain tissue of patients with normal renal function. Kanda et al[4] first reported abnormally increased T1 signal intensity (SI) in the dentate nucleus (DN) and globus pallidus (GP) on unenhanced T1-weighted sequences after repeated injections of linear GBCA. These findings were later replicated[5–7] and extended to other brain structures: posterior thalamus,[8] colliculi, red nucleus, putamen, and substantia nigra (SN).[9] Furthermore, post mortem studies using inductively coupled plasma mass spectroscopy revealed a positive correlation between the cumulative GBCA dose, SI in T1-weighted MR images, and gadolinium concentration in neuronal tissues (DN, GP, and thalamus), providing direct evidence for the relationship between linear GBCA and subsequent neuronal tissue deposition.[8,10]

Despite the well-established link between abnormally increased SI in the brain and accumulative GBCAs exposure, the exact spatiotemporal pattern of gadolinium deposition has not been addressed yet. For example, multiple studies compared the SI between the patients' baseline and the last MR examination[4,7,8,11] or they assessed the SI change after different injection number intervals,[9] but no continuous assessment of the SI change over consecutive GBCA exposure has been performed at a subject level. Moreover, previous studies have used different reference areas to normalize the region of interest's (ROI) SI, for example, the thalamus to normalize the values of GP, pons or medial cerebral peduncle for the DN, SN, colliculi, and red nucleus,[4,5,7,9,11] or cerebellar white matter for the DN,[12] making a comparison between ROIs impossible. As such, it remains unclear whether certain brain areas are more prone to accumulate gadolinium.

The purpose of this study was to map the rate of SI increase over consecutive GBCA administrations across multiple deep brain structures. This was performed by a longitudinal study where each patient was followed from the first baseline through each of the 10 consecutive gadodiamide-enhanced MR imaging examinations, using quantitative assessment of SIs and a single reference tissue for ROIs normalization.

## MATERIALS AND METHODS

The study was approved by the Ethics Committee of canton Vaud (CER-VD, reference no. 2017–00959). Due to the retrospective type of the study, the informed consents have been waived.

### Patients

The patient's data have been extracted from our hospital database between December 1998 and February 2008, as this was the period when gadodiamide (Omniscan; GE Healthcare, Chalfont Saint Giles, United Kingdom) was administered routinely as the only MR imaging contrast agent in the hospital. We extracted the data of 83 patients who had undergone first 10 successive contrast-enhanced MR examinations and an unenhanced T1 imaging of the 11th contrast-enhanced MR examination in the given period, and were at least 18 years old at the time of the first MR examination. This sample did not include patients with multiple sclerosis, metabolic disease, metal toxicity, congenital cerebral malformations, or intracranial infections. We excluded

**TABLE 1.** Patient Characteristics

| Total No. Patients | 30 |
|---|---|
| Mean age (at the baseline MRI) | 42.97 (19–67, SD = 11.81) |
| Sex | |
|    M | 18 |
|    F | 12 |
| Mean cumulative dose (mL per 10 injections) | 144.73 (90–210, SD = 26.60) |
|    (mmol Gd per 10 injections) | 72.37 (45–105, SD = 13.30) |
| Mean interval between gadodiamide administrations, wk | 12.6 (0–61, SD = 11.1) |
| Mean total interval between the first and 11th gadodiamide* administration, wk | 141.9 (65–292, SD = 62.2) |
| Tumor | |
|    WHO grade II (oligodendroglioma, oligoastrocytoma) | 9 |
|    WHO grade III (anaplastic astrocytoma) | 4 |
|    WHO grade IV (glioblastoma) | 10 |
|    other (germinoma, brain metastasis, meningioma, cavernomatosis) | 7 |
| Surgery | 29 |
|    Chemotherapy | 22 |
|    Radiotherapy | |
|       Partial | 22 |
|       Radiosurgery | 2 |
| eGFR (mL/min per 1.73 m$^2$) | |
|    >90 | 15 |
|    90–60 | 13 |
|    30–60 | 1 |

*Each MRI session included first an unenhanced imaging, followed by an administration of gadodiamide. The interval between the baseline and the last measure is therefore identical to the interval between the first and the 11th gadodiamide administration.

MRI indicates magnetic resonance imaging; WHO, World Health Organization; eGFR indicates estimated glomerular filtration rate, using CKD-EPI formula.

patients with bilateral lesions involving one or more predefined ROIs (n = 5) and those patients who had a previous MR examination at an outside hospital due to a possible exposure to other GBCAs (n = 48). Demographic data and relevant clinical information were collected from the patients' electronic medical records. Our final sample comprised 30 patients (12 women, 18 men; age range, 19–67 years, M = 43, SD = 11.6 years). The patients' demographic and clinical information is displayed in Table 1.

## Imaging Protocols

All patients in the final sample underwent multiple MR imaging of the brain, which included unenhanced T1-weighted sagittal spin echo sequence of entire brain. The majority of MR examinations were performed with a 1.5 T Siemens scanner (Vision or Symphony; Siemens Healthcare, Erlangen, Germany); however, some were acquired with a Philips scanner (Intera 3 T; Philips Healthcare, Best, the Netherlands) or Siemens 3 T scanner (Trio or Verio). The image data acquired on the Phillips scanner (7%) or 3 T Siemens scanners (0.6%) were omitted from the analyses. At our institution, a standard dose of 0.1 mmol Gd/kg of gadodiamide (Omniscan, GE Healthcare) was administered at every contrast-enhanced MR examination.

The measurements were performed on the unenhanced sagittal T1-weighted spin echo sequences (repetition time/echo time, 450–524/12–14 milliseconds; matrix size, 256 × 256 or 512 × 512; slice thickness, 5 mm) acquired during the standard imaging protocols.

## Imaging Analysis

The MR images were reviewed and measured on the institutional PACS viewing software (VuePacs; Carestream, Rochester, NY). Quantitative image analyses were performed independently by 2 observers: a radiologist with 2 years of experience and a neuroscientist with 1 year of experience, who manually traced regions of interest on the following ROIs: DN, GP, anterior putamen, posterior thalamus (pulvinar), ventral posterior nucleus of the thalamus (VPN), SN, superior colliculus (SC), WM (anterior corona radiata), and the pons. The placement of ROIs is shown in Figure 1. All the ROIs were drawn contralateral to the side of the tumor (contralesional, healthy side), except when a proper placement on the SC was not possible due to the interslice gap, the ROI was placed on the ipsilesional side. Corresponding T2-weighted images were used to guide the placement of the ROIs. The pons was used as a reference tissue to account for intrasubject and intersubject intensity variations and MR scanner differences. We calculated the ratios by dividing the mean value of the ROI's SI by the mean value of the pons.
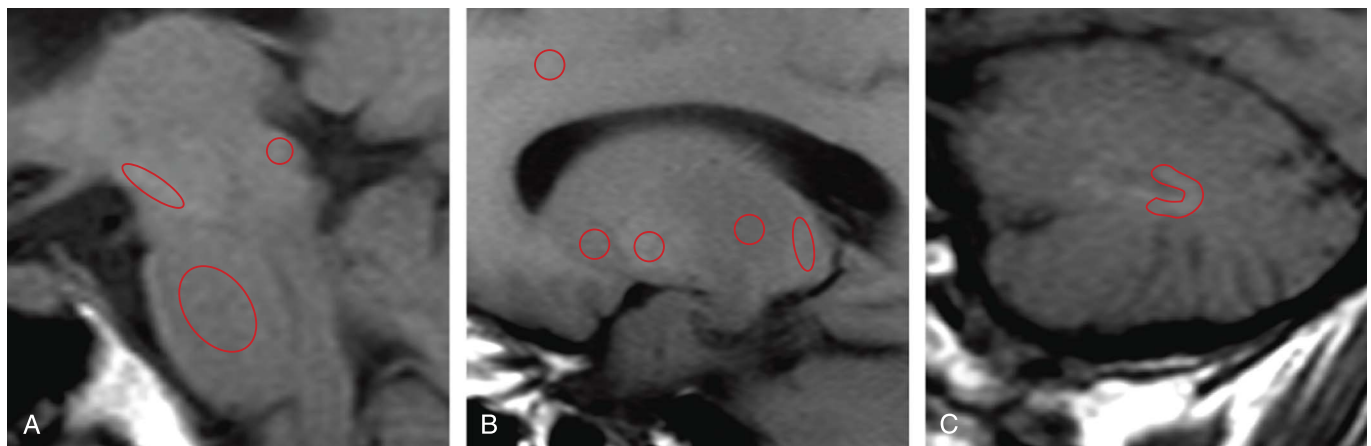


**FIGURE 1.** Placement of the ROIs. Three sagittal slices show the ROIs on unenhanced T1-weighted spin echo images. The ROIs were placed on (from left to right): (A) substantia nigra, superior colliculus, and pons; (B) white matter of anterior corona radiata, putamen, globus pallidus, ventral posterior nucleus of the thalamus, and pulvinar; and (C) dentate nucleus.

In contrast to previous studies[4,5,7,9,11] where adjacent tissues were used for normalization (eg, thalamus for GP, and pons for the DN), we used the pons as the only reference tissue for all our ROIs. This enabled us to directly compare the rate of signal increase between the ROIs.

## Clinical Data Analysis

We evaluated age, sex, diagnosis, chemotherapy, and radiotherapy treatments for all selected patients. Based on the World Health Organization grading of central nervous system tumors,[13] the diagnoses were grouped into the following 4 categories: (*a*) grade II tumors, (*b*) grade III tumors, (*c*) grade IV tumors, and (*d*) other tumors. We assessed whether the patients were treated with whole-brain radiotherapy, tumor-selected radiotherapy, or stereotactic radiosurgery.

## Statistical Analysis

Statistical analyses were conducted using statistical software (R, version 3.4.1; R Foundation for Statistical Computing, Vienna, Austria). To account for the missing data, subject-level variability, and longitudinal data dependencies, we analyzed our data with linear mixed effects models using the statistical package lme4.[14]

The number of gadodiamide administrations and covariates (age at the baseline MR examination [in years], sex, diagnosis, time elapsed since the respective and previous MR examination [in weeks], radiotherapy, and chemotherapy) were entered as fixed effects without interaction terms. Intercepts for subjects and by-subject slopes for the effect of the number of injections were entered as random effects. For each normalized ROI, we built a minimal model including only the random subject intercept. The best model was then selected by forward stepwise addition of predictors, using $\chi^2$ tests on log likelihood ratios to compare different models and assess the model fit. The *P* values of the predictors in the final model were calculated based on Satterthwaite approximation using the lmerTest package.[15]

In addition, to assess a possible logarithmic relationship between the number of injections and SI ratio, we compared, for each ROI, the linear model with the model where the predictor (number of gadodiamide administrations) was logarithmically transformed with the natural logarithm. The statistical comparisons of the model fit were performed with Vuong test[16] for non-nested models selection.

To evaluate potential differences between the ROIs in their signal ratio increase rate across successive gadodiamide administrations, we compared the average slopes of the ROIs through pairwise comparisons, using lstrends function of the lsmeans R package.[17] Tukey method was used to correct the *P* values for multiple comparisons.

## RESULTS

### Patients

All our patients, except one, underwent surgical removal of the tumor, 22 patients were treated with chemotherapy (73%), none of our patients underwent a whole-brain radiation therapy, and 22 patients underwent gamma-knife stereotactic radiosurgery or other tumor selective radiation therapy (73%). All of the selected patients had glomerular filtration rate values above 30 mL/min per square meter. Nine patients (30%) had grade II brain tumors (oligodendroglioma and oligoastrocytoma), 4 patients (13.3%) grade III tumors (anaplastic astrocytoma), 10 patients (33.3%) grade IV tumors (glioblastoma), and 7 patients (23.3%) other type of lesions (germinoma, brain metastasis, meningioma, or cavernomatosis). The mean time interval between 2 successive gadodiamide administrations was $12.6 \pm 11.1$ weeks, ranging from 0 to 61 weeks, and the mean interval between the first gadodiamide injection and the patient's last unenhanced MR image used in the analysis was $141.9 \pm 62.2$ weeks, ranging from 65 to 292 weeks. The mean accumulated contrast dose for 10 gadodiamide administrations was 144.73 mL (72.37 mmol Gd) $\pm$ 26.60 mL (13.30 mmol Gd), ranging from 90 to 210 mL (45 to 105 mmol Gd).

### Effect of Gadodiamide Exposure on Unenhanced T1-Weighted Signal Intensity

Compared with previous studies, which either analyzed the signal change between the baseline and the last GBCA administration[4,5,7,8,11,18,19] or analyzed the signal change after different administration number intervals,[9] we here quantitatively assessed the T1-weighted signal at the baseline and after every of the first 10 GBCA administrations for 8 different brain structures to establish a detailed temporal and spatial pattern of the gadolinium-related signal increase.

Statistical analyses showed that the SI significantly increased with the number of gadodiamide administrations in all the selected deep brain structures but not in the WM. The fastest SI increase was observed in the DN ($P < 0.001$), followed by GP ($P < 0.001$), putamen ($P < 0.001$), pulvinar ($P < 0.001$), SC ($P < 0.001$), SN ($P < 0.001$), and VPN ($P = 0.0117$). No significant SI increase was observed in the WM ($P = 0.055$). Moreover, we found a significant positive effect of age on the SI of the GP ($P = 0.0127$) and the putamen ($P = 0.037$). Detailed statistical results are presented in Table 2. Scatter plots showing the increase in SI ratios are presented in Figure 2. An example of the signal increase on unenhanced T1-weighted MR images before any and

**TABLE 2.** F Tests and Related Statistical Values for the Predictors in the Final Models

| ROI | Predictor | *df* | F | *P* | B | 95% CI |
|---|---|---|---|---|---|---|
| DN | No. Gd administrations | 1, 252.9 | 48.5 | <0.001 | 0.010 | 0.0075, 0.0134 |
| GP | No. Gd administrations | 1, 96.3 | 19.2 | <0.001 | 0.0068 | 0.0037, 0.0099 |
|  | age | 1, 95.9 | 6.4 | 0.0127 | 0.0011 | 0.0003, 0.0020 |
| Put | No. Gd administrations | 1, 95 | 19.7 | <0.001 | 0.0063 | 0.0035, 0.0091 |
|  | age | 1, 98.8 | 8.8 | 0.037 | 0.0012 | 0.0004, 0.0020 |
| Pul | No. Gd administrations | 1, 50.4 | 14.5 | <0.001 | 0.0062 | 0.0030, 0.0095 |
| SC | No. Gd administrations | 1, 66.4 | 34.3 | <0.001 | 0.0057 | 0.0035, 0.0078 |
| SN | No. Gd administrations | 1, 245.1 | 11.2 | <0.001 | 0.0034 | 0.0014, 0.0053 |
| VPN | No. Gd administrations | 1, 251.6 | 6.5 | 0.0117 | 0.0031 | 0.0007, 0.0056 |
| WM* | No. Gd administrations | 1, 251.6 | 3.7 | 0.0550 |  |  |

*Inclusion of the predictor (number of gadodiamide administrations) did not significantly improve the simpler model.

ROI indicates region of interest; CI, confidence interval; DN, dentate nucleus; GP, globus pallidus; Pul, pulvinar; Put, putamen; SC, superior colliculus; SN, substantia nigra; VPN, ventral posterior nucleus of the thalamus; WM, white matter.

**FIGURE 2.** Scatter plots for the SI ratios (ROI/pons) of the ROIs across 10 successive gadodiamide administrations. Each data point presents a ratio of a patient at the respective gadodiamide administration. DN indicates dentate nucleus; GP, globus pallidus; Pul, pulvinar; Put, putamen; SC, superior colliculus; SN, substantia nigra; VPN, ventral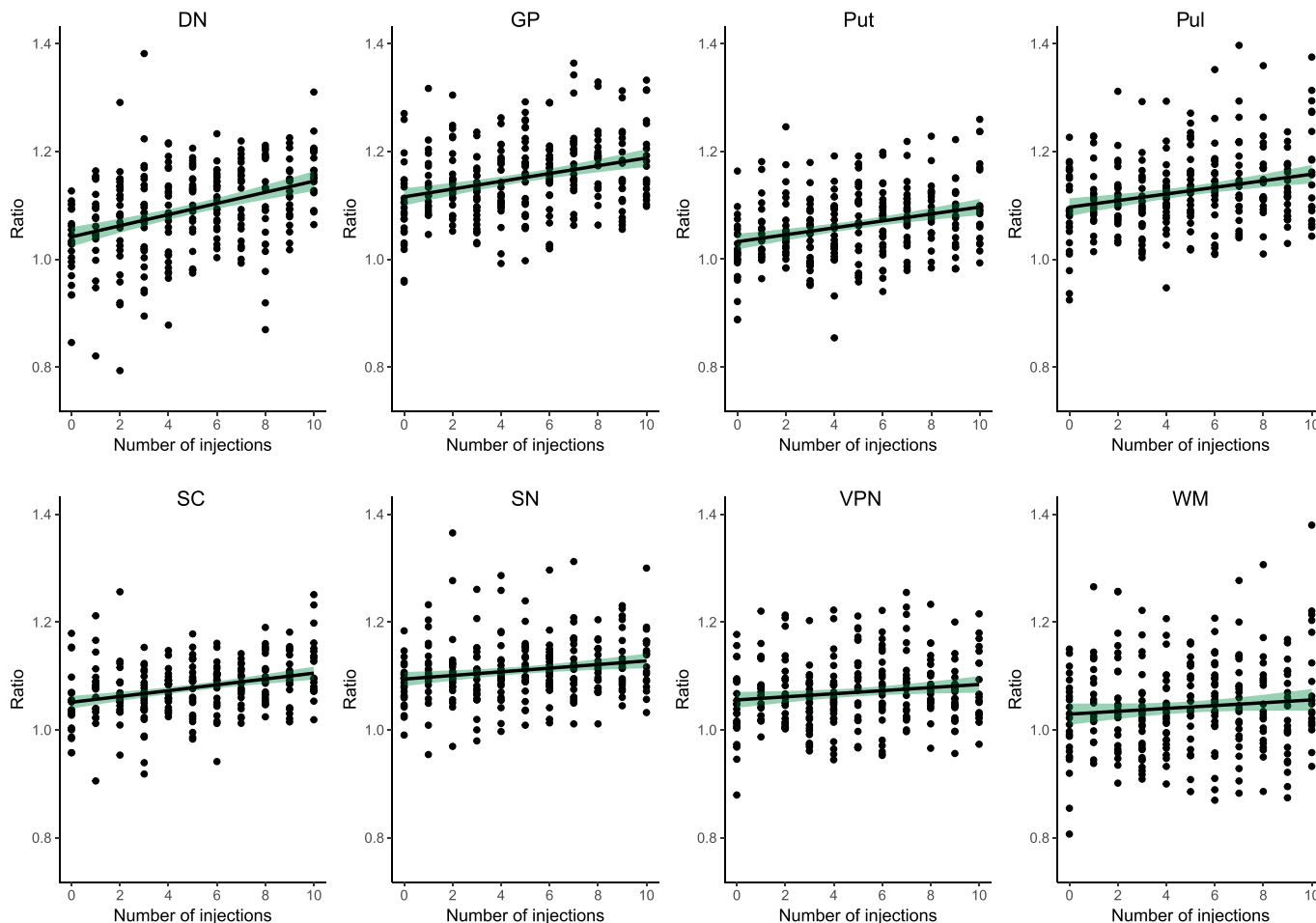 posterior nucleus of the thalamus; WM, white matter. The shaded areas represent 95% confidence interval of the regression line.

after the 10th gadodiamide administration in a single patient is demonstrated in Figure 3.

Statistical analyses showed that the logarithmic regression of the SI ratios on the number of injections did not show a better fit to the data as compared with the linear regression for all the ROIs (all $P > 0.05$).

The comparison of the slopes (average fitted lines of ratio across the number of gadodiamide administrations) between the ROIs showed that the DN slope was significantly steeper than the slopes of SN, VPN, and WM (all $P < 0.05$). Other pairwise comparisons were not statistically significant ($P > 0.05$).

## DISCUSSION

We analyzed retrospective longitudinal MR imaging data of brain lesion patients, who had received at least 10 consecutive doses of gadodiamide, a linear nonionic gadolinium contrast agent. We demonstrated that the T1-weighted hyperintensity ratios increased gradually, that they were positively correlated with the number of received gadodiamide administrations, and that the rate of the observed increase was nonuniform across different deep brain nuclei. By using a single reference tissue, we were able to compare the increase rate of the signal

across all our ROIs. We showed that the increase is the most pronounced in the DN, followed by GP, putamen, pulvinar, SC, SN, and VPN.

We speculate that the observed differences between the brain tissues in their capacity to accumulate gadolinium might be explained by their different intrinsic content of metal cations. A prominent explanation of the gadolinium deposition is the transmetallation reaction, during which the endogenous metallic cations compete for the ligand in the chelate and cause dechelation of the gadolinium ion, which subsequently binds to other biomolecules such as phosphates.[20–22] As proposed by Swaminathan,[23] endogenous level of iron in the brain tissue might play an important role in the process of transmetallation and gadolinium retention. In fact, the structures, which are prone to accumulate gadolinium (specifically DN, GP, putamen, SN, and red nucleus), have been often identified as structures intrinsically rich in iron[24–26] and as targets for iron accumulation related to neurodegenerative diseases.[27] Multiple administration of linear GBCA has also been linked to an increase in iron mobilization and serum ferritin levels,[23] and to increased iron accumulation in autopsy tissue of nephrogenic systemic fibrosis patients.[28] Moreover, an in vivo study on rats who received a cumulated dose of 12 mmol/kg of gadodiamide over 5 weeks showed that the gadolinium concentration positively correlated with the distribution of iron in the deep brain structures.[29] Alternative to the transmetallation explanation, the correlation
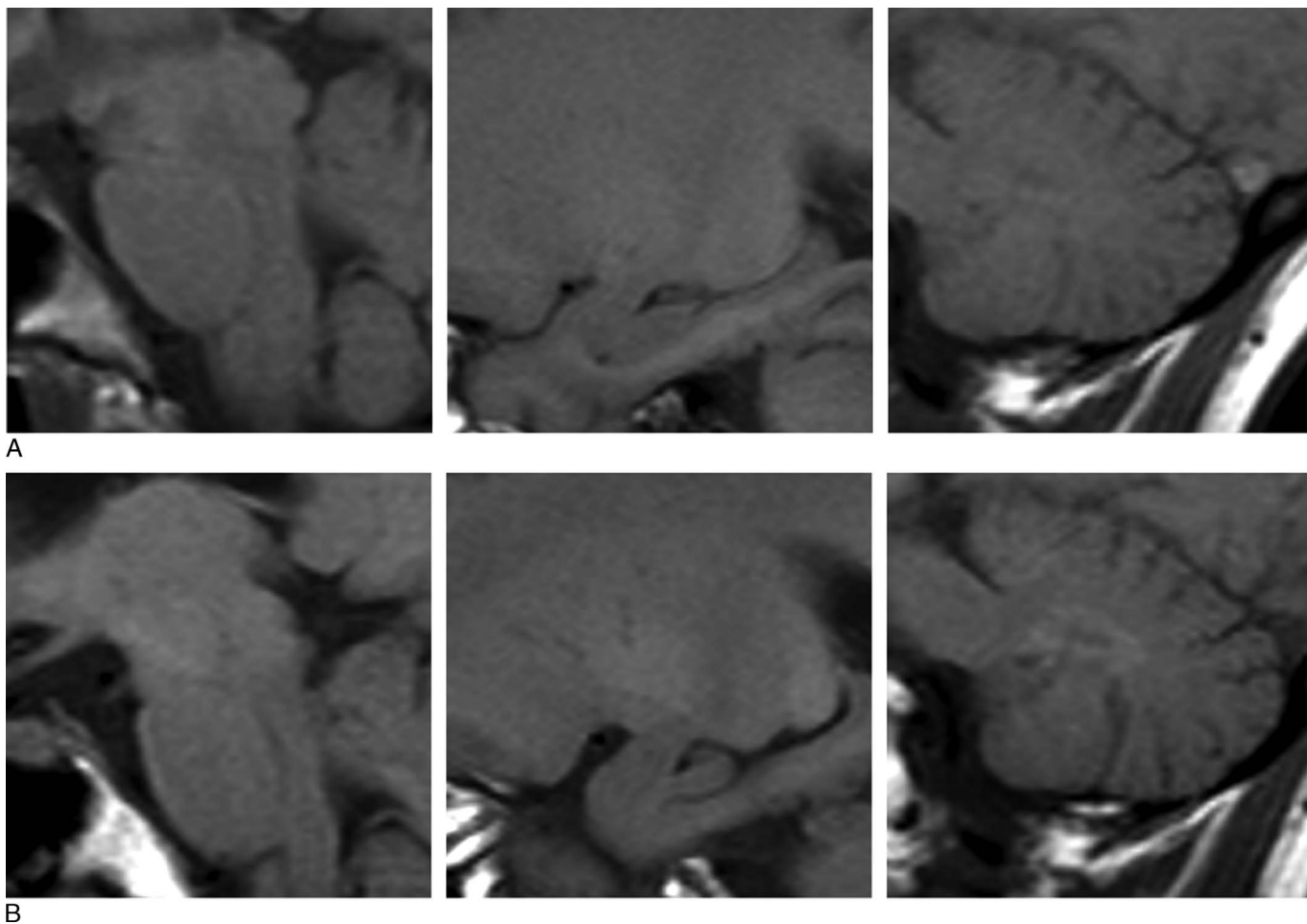
**FIGURE 3.** MR images of a woman experiencing right frontal glioblastoma: (A) unenhanced T1-weighted images before the first gadodiamide administration and (B) after the 10th administration showing visible increase of the signal intensity in the (from left to right) substantia nigra, colliculi, globus pallidus, pulvinar, and dentate nucleus.

between iron and gadolinium content concentrations might be due to a possibility that both metals use the same pathway of accumulation in the brain.[29] Besides iron, the role of zinc,[30] calcium,[31] and phosphate[2,32] in the dechelation and tissue deposition has been suggested.

Our analyses revealed that besides the number of gadodiamide administrations, an increased age also significantly contributed to the augmentation of the SI in the GP and putamen. This finding might indicate a confounding effect of the age-related accumulation of other metallic cations in these structures, potentially contributing to the observed SI enhancement. The putamen and GP are 2 of the deep brain structures with high susceptibility to accumulate iron with advanced age.[24,27] A recent meta-analysis of 20 studies on non-heme iron concentration in the subcortical nuclei showed that the largest age-related differences occur in the putamen but the smallest in GP.[33] However, iron accumulation in GP steeply increases in the first life decade and reaches a plateau in early adulthood.[34] The age heterogeneity of our sample might explain why we have not observed the aforementioned age-related differences in signal increase between the 2 nuclei. On the other hand, the putamen and GP are also susceptible to accumulate pathological levels of manganese and copper, and physiological calcification, which all result in hyperintense T1-weighted signal.[35] These confounding effects should be thus taken into account when interpreting the gadolinium deposition data, specifically in the pediatric population where the basal ganglia's normal iron concentrations augment drastically during the childhood.[25,34] The exact mechanism of how gadolinium enters the brain is not fully understood; however, the results of the study using inductively coupled plasma mass spectroscopy and transmission electron microscopy suggest that the GBCAs cross an intact blood-brain barrier and deposit in the neural interstitium.[8] Our data support this notion as we found dose-dependent SI increase in the structures, which were measured on the contralesional site, and had therefore presumably intact blood-brain barrier. However, gadolinium could also enter into the neural interstitium by a different pathway. An alternative but prominent explanation for the gadolinium entry in the brain is by crossing the blood–cerebrospinal fluid barrier through choroid plexus and consequently penetrating into the brain parenchyma either by diffusion or through a glymphatic system[36–38]—a recently hypothesized waste clearance system of the brain.[39] The observed signal increase across the successive administrations of gadodiamide is most probably affected by a complex interaction of multiple factors, including the stability of the gadolinium contrast, metal content of the tissue, and possibly the tissue's anatomical proximity to the cerebrospinal fluid.

In addition, the time lapse between 2 successive gadodiamide administrations did not significantly affect the normalized SI, and the SI increase was linear, demonstrating that the washout during the first 10 gadodiamide administrations is not very likely, or it occurs in amounts we were not able to detect with our methodology. However, we cannot conclude from the present data whether such linear increase

persists after the 10th GBCA administration or whether a nonlinear trend occurs with larger number of injections, possibly indicating an elimination of accumulated gadolinium.

Our detailed temporal analysis using single reference tissue revealed that the increase is gradual and, importantly, that it occurs before it can be detected by visual inspection of the MR images. It is therefore possible to see early SI enhancement also in the structures where the gadolinium retention after a single dose of gadodiamide was detected with post mortem inductively coupled plasma mass spectroscopy analysis[8,40] or in the structures that have been previously used as a reference tissue, for example, thalamus.[4,5,7,9,18] As such, our results contrast and complement previous qualitative studies, stating that the increase in the DN is visually observed by a trained radiologist only after about 5 administrations of linear GBCA[5,41] and in several other structures (putamen, thalamus, and SC) only after 12 or 24 injections.[9] Also, when compared with Errante et al,[5] who used 6 GBCA administrations as a qualitative cutoff for their DN/pons SI subgroup analysis, we observed no inflection of the DN/pons ratio curve before or after 6 injections, making the justification of the split-off questionable.

Moreover, in the previous studies different reference tissues were used for normalization of the nuclei's T1-weighted signal. Authors most commonly used adjacent thalamus to normalize the values of GP,[4,5,7,9,18] and pons or medial cerebral peduncle for the DN, SN, colliculi, and red nucleus.[4,5,7,9,18] Despite a recent autopsy report of low levels of gadolinium detected in the pons,[8] we nevertheless used this structure for the normalizing reference as it has a central position in the brain and is therefore less subjected to the magnetic field inhomogeneity. Being a relatively large structure, it also reduces the risk of partial volume effect during the measurement, as it is a mix of gray and white matter and is not like cerebrospinal fluid susceptible to noise.[12]

Due to a low spatial resolution of our MR images, we were not able to measure several other deep brain structures, such as the caudate nucleus, red nucleus, nucleus accumbens, caudolenticular gray bridges, or discriminate between different substructures of putamen or thalamus or the adjacent nuclei (subthalamic nucleus, lateral, and medial geniculate). We speculate that using higher-resolution imaging would identify a more extensive and diffuse pattern of accumulation. For example, the post mortem specimen autopsy using inductively coupled plasma mass spectroscopy, detected low levels of gadolinium also in the cerebellar white matter, frontal lobe white matter, and frontal lobe cortex,[41] showing that the distribution of the gadolinium is not only limited to the deep brain nuclei.

In conclusion, this is the first longitudinal retrospective study that systematically quantified the spatiotemporal pattern of gadolinium-related T1-weighted signal increase in the brain. We showed that multiple consecutive administration of gadodiamide is associated with an increase in T1-weighted hypersignal on unenhanced MR images, displaying a gradual and nonuniform pattern across different deep brain nuclei.

## REFERENCES

1. Lancelot E. Revisiting the pharmacokinetic profiles of gadolinium-based contrast agents. *Invest Radiol*. 2016;51:691–700.
2. Frenzel T, Lengsfeld P, Schirmer H, et al. Stability of gadolinium-based magnetic resonance imaging contrast agents in human serum at 37°C. *Invest Radiol*. 2008; 43:817–828.
3. Marckmann P, Skov L, Rossen K, et al. Nephrogenic systemic fibrosis: suspected causative role of gadodiamide used for contrast-enhanced magnetic resonance imaging. *J Am Soc Nephrol*. 2006;17:2359–2362.
4. Kanda T, Ishii K, Kawaguchi H, et al. High signal intensity in the dentate nucleus and globus pallidus on unenhanced T1-weighted MR images: relationship with increasing cumulative dose of a gadolinium-based contrast material. *Radiology*. 2014;270:834–841.
5. Errante Y, Cirimele V, Mallio CA, et al. Progressive increase of T1 signal intensity of the dentate nucleus on unenhanced magnetic resonance images is associated with cumulative doses of intravenously administered gadodiamide in patients with normal renal function, suggesting dechelation. *Invest Radiol*. 2014;49:685–690.
6. Cao Y, Huang DQ, Shih G, et al. Signal change in the dentate nucleus on T1-weighted MR images after multiple administrations of gadopentetate dimeglumine versus gadobutrol. *Am J Roentgenol*. 2016;206:414–419.
7. Ramalho J, Castillo M, AlObaidy M, et al. High signal intensity in globus pallidus and dentate nucleus on unenhanced T1-weighted MR images: evaluation of two linear gadolinium-based contrast agents. *Radiology*. 2015;276:836–844.
8. McDonald RJ, McDonald JS, Kallmes DF, et al. Intracranial gadolinium deposition after contrast-enhanced MR imaging. *Radiology*. 2015;275:772–82.
9. Zhang Y, Cao Y, Shih GL, et al. Extent of signal hyperintensity on unenhanced T1-weighted brain MR images after more than 35 administrations of linear gadolinium-based contrast agents. *Radiology*. 2016;282:516–525.
10. Kanda T, Fukusato T, Matsuda M, et al. Gadolinium-based contrast agent accumulates in the brain even in subjects without severe renal dysfunction: evaluation of autopsy brain specimens with inductively coupled plasma mass spectroscopy. *Radiology*. 2015;276:228–232.
11. Radbruch A, Weberling LD, Kieslich PJ, et al. Gadolinium retention in the dentate nucleus and globus pallidus is dependent on the class of contrast agent. *Radiology*. 2015;275:783–791.
12. Roberts DR, Chatterjee AR, Yazdani M, et al. Pediatric patients demonstrate progressive T1-weighted hyperintensity in the dentate nucleus following multiple doses of gadolinium-based contrast agent. *Am J Neuroradiol*. 2016;37:2340 LP-2347. Available at: http://www.ajnr.org/content/37/12/2340.abstract.
13. Louis DN, Ohgaki H, Wiestler OD, et al. The 2007 WHO classification of tumours of the central nervous system. *Acta Neuropathol*. 2007;114:97–109.
14. Douglas B, Maechler M, Bolker B, et al. Fitting linear mixed-effects models using lme4. *J Stat Softw*. 2015;67:1–48.
15. Kuznetsova A, Brockhoff PB, Christensen RH. lmerTest package: tests in linear mixed effects models. *J Stat Softw*. 2017;82:1–26.
16. Vuong QH. Likelihood ratio tests for model selection and non-nested hypotheses. *Econometrica*. 1989;57:307–333.
17. Lenth RV. Least-squares means: the R package lsmeans. *J Stat Softw*. 2016;69.
18. Radbruch A, Weberling LD, Kieslich PJ, et al. High-signal intensity in the dentate nucleus and globus pallidus on unenhanced T1-weighted images: Evaluation of the macrocyclic gadolinium-based contrast agent gadobutrol. *Invest Radiol*. 2015;50:805–810.
19. Radbruch A, Weberling LD, Kieslich PJ, et al. Intraindividual analysis of signal intensity changes in the dentate nucleus after consecutive serial applications of linear and macrocyclic gadolinium-based contrast agents. *Invest Radiol*. 2016;51:683–690.
20. Idée J-M, Port M, Raynal I, et al. Clinical and biological consequences of transmetallation induced by contrast agents for magnetic resonance imaging: a review. *Fundam Clin Pharmacol*. 2006;20:563–576.
21. Corot C, Idee JM, Hentsch AM, et al. Structure-activity relationship of macrocyclic and linear gadolinium chelates: investigation of transmetallation effect on the zinc-dependent metallopeptidase angiotensin-converting enzyme. *J Magn Reson Imaging*. 1998;8:695–702.
22. Tweedle MF, Wedeking P, Kumar K. Biodistribution of radiolabeled, formulated gadopentetate, gadoteridol, gadoterate, and gadodiamide in mice and rats. *Invest Radiol*. 1995;30:372–380.
23. Swaminathan S. Gadolinium toxicity: iron and ferroportin as central targets. *Magn Reson Imaging*. 2016;34:1373–1376.
24. Bilgic B, Pfefferbaum A, Rohlfing T, et al. MRI estimates of brain iron concentration in normal aging using quantitative susceptibility mapping. *Neuroimage*. 2012;59:2625–2635.
25. Aoki S, Okada Y, Nishimura K, et al. Normal deposition of brain iron in childhood and adolescence: MR imaging at 1.5 T. *Radiology*. 1989;172:381–385.
26. Haacke EM, Ayaz M, Khan A, et al. Establishing a baseline phase behavior in magnetic resonance imaging to determine normal vs. abnormal iron content in the brain. *J Magn Reson Imaging*. 2007;26:256–264.
27. McNeill A, Chinnery PF. Neurodegeneration with brain iron accumulation. *Handb Clin Neurol*. 2011;100:161–172.
28. Swaminathan S, High WA, Ranville J, et al. Cardiac and vascular metal deposition with high mortality in nephrogenic systemic fibrosis. *Kidney Int*. 2008;73:1413–1418.
29. Rasschaert M, Emerit A, Fretellier N, et al. Gadolinium retention, brain T1 hyperintensity, and endogenous metals: a comparative study of macrocyclic versus linear gadolinium chelates in renally sensitized rats. *Invest Radiol*. 2018;53:328–337.
30. Greenberg SA. Zinc transmetallation and gadolinium retention after MR imaging: case report. *Radiology*. 2010;257:670–673.
31. Idée JM, Berthommier C, Goulas V, et al. Haemodynamic effects of macrocyclic and linear gadolinium chelates in rats: role of calcium and transmetallation. *Biometals*. 1998;11:113–123.

32. Robic C, Catoen S, De Goltstein M-C, et al. The role of phosphate on Omniscan® dechelation: an in vitro relaxivity study at pH 7. *Biometals*. 2011;24:759–768.

33. Daugherty A, Raz N. Age-related differences in iron content of subcortical nuclei observed in vivo: a meta-analysis. *Neuroimage*. 2013;70:113–121.

34. Aquino D, Bizzi A, Grisoli M, et al. Age-related iron deposition in the basal ganglia: quantitative analysis in healthy subjects. *Radiology*. 2009;252: 165–172.

35. Zaitout Z, Romanowski C, Karunasaagarar K, et al. A review of pathologies associated with high T1W signal intensity in the basal ganglia on magnetic resonance imaging. *Pol J Radiol*. 2014;79:126–130.

36. Jost G, Frenzel T, Lohrke J, et al. Penetration and distribution of gadolinium-based contrast agents into the cerebrospinal fluid in healthy rats: a potential pathway of entry into the brain tissue. *Eur Radiol*. 2017;27:2877–2885.

37. Taoka T, Jost G, Frenzel T, et al. Impact of the glymphatic system on the kinetic and distribution of gadodiamide in the rat brain: observations by dynamic MRI and

38. effect of circadian rhythm on tissue gadolinium concentrations. *Invest Radiol*. 2018;53:529–534.

38. Jost G, Lenhard DC, Sieber MA, et al. Signal increase on unenhanced T1-weighted images in the rat brain after repeated, extended doses of gadolinium-based contrast agents: comparison of linear and macrocyclic agents. *Invest Radiol*. 2016;51:83–89.

39. Iliff JJ, Wang M, Liao Y, et al. A paravascular pathway facilitates CSF flow through the brain parenchyma and the clearance of interstitial solutes, including amyloid β. *Sci Transl Med*. 2012;4:147ra111.

40. Murata N, Gonzalez-Cuyar LF, Murata K, et al. Macrocyclic and other non-group 1 gadolinium contrast agents deposit low levels of gadolinium in brain and bone tissue: preliminary results from 9 patients with normal renal. *Invest Radiol*. 2016;51:447–453.

41. Kanda T, Oba H, Toyoda K, et al. Brain gadolinium deposition after administration of gadolinium-based contrast agents. *Jpn J Radiol*. 2016;34:3–9.